Investigating the Utility of Machine Learning Algorithms in Glycan-Specificity in Influenza A

Sezen Zeynep Sümer

Supervisor: David Burke

Department/Centre address: King's College London, Guy's Campus

This report has been submitted in part-fulfilment of the requirements for the MSc in Microbiome in Health and Disease at King's College London

Date of Submission: 30th September, 2024

Abstract

Zoonotic viruses pose a significant global threat, as exemplified by recent pandemics such as the 2009 A/H1N1 influenza and the 2020 SARS-CoV2 pandemic, which collectively caused millions of deaths worldwide [1,2]. To better prevent and manage future global pandemics, it is crucial to identify viruses in animal hosts and predict their zoonotic potential. Among these threats, avian influenza viruses (AIVs), especially the H5 and H7 subtypes, are of particular concern due to their increasing spread and associated human fatalities [3–7]. The hemagglutinin (HA) protein, central to viral entry by binding to sialic acid (SA) receptors on host cells, plays a pivotal role in determining host specificity in the influenza virus [8–12]. Insights gained from the well-characterised H3 subtype, which has caused infections in both avian and human hosts, may enhance our understanding of the binding capabilities of subtypes with potential pandemic risks, such as the H5 and H7 subtypes. Machine learning (ML) algorithms, which have demonstrated significant promise in predicting ligand-protein interactions, offer a powerful tool for assessing zoonotic potential [13–19]. This research aims to assess selected ML methods for predicting glycan specificity in avian influenza and decode feature importance, utilising publicly available viral sequence data. The goal is to enhance predictive accuracy, contributing to the early identification and mitigation of potential zoonotic threats, and thereby strengthening global preparedness against emerging viral pandemics.

1. Introduction

1.1 Background

Zoonoses, which are diseases transmitted from vertebrate animals to humans, account for 75% of all emerging infectious diseases [20–22]. Among zoonotic diseases, avian influenza poses a significant emerging threat due to its ability to cross species barriers and potentially cause pandemics. Historical pandemics, including the Spanish, Asian, Hong Kong, and Swine flu, were all caused by different subtypes of the influenza A virus (IAV). Influenza A viruses are classified based on their two surface proteins, hemagglutinin (HA) and neuraminidase (NA), of which 16 HA and 9 NA subtypes have been identified across various avian species [23,24]. Wild birds and waterfowl are natural reservoirs for nearly all IAV subtypes, and these viruses occasionally spill over to other species, including pigs, humans, and other mammals, leading to potential outbreaks and sustained transmission. For example, the 1957–1958 Asian flu pandemic, caused by the H2N2 subtype, is believed to have originated from an avian host. Similarly, the 1968 Hong Kong flu pandemic was triggered by the H3N2 subtype, which emerged as a descendant of H2N2, also having avian origins. These pandemics resulted in estimated fatalities of 1.1 million and 1 million people, respectively [25–28].

Among these subtypes, the H3 subtype has established itself in both human and avian hosts through distinct evolutionary pathways. In humans, the H3N2 subtype emerged during the 1968 Hong Kong flu pandemic and has since circulated as a seasonal influenza strain, undergoing frequent antigenic drift to evade immune responses [24,28–31]. This makes it a persistent cause of seasonal flu epidemics. The genetic flexibility and reassortment of H3 strains across species enable the subtype to maintain its presence in both human and avian reservoirs, posing an ongoing zoonotic risk.

In contrast to the established H3 subtype, highly pathogenic H5 and H7 subtypes present a more recent and pressing global health challenge. These subtypes have caused severe outbreaks in poultry and sporadic human infections, raising alarms due to their high mortality rates—exceeding 50% in some cases[7]. Although primarily avian in nature, H5 and H7 have demonstrated the ability to cross into humans, sparking concerns about their potential to adapt for efficient human-to-human transmission. These strains, especially H5N1 and H7N9, are closely monitored due to their potential to mutate and cause widespread human transmission. From January 2003 to July 2024, H5 has resulted in 1,237 human cases including 678 deaths, while H7 has caused 1,680 cases including 617 deaths, with mortality rates of 54.8% and 36.7% [7,32–36].

Current surveillance data indicate that human infections primarily occur through direct contact with infected poultry or contaminated environments, with human-to-human transmission being extremely rare [7,24,32,37]. To prevent the possibility of these viruses acquiring the capability for sustained human-to-human transmission, it is crucial to understand the underlying mechanisms that drive spillover infections.

1.2 Host Specificity and Mutations in the HA Protein

The surface protein hemagglutinin has been previously identified as a crucial determinant of host specificity and plays a fundamental role in the virus life cycle by binding to the SA receptors on host cell surfaces, initiating the infection process [12,38,39]. Initially synthesised as a precursor, HA0, this protein consists of two subunits: HA1, which contains the receptor binding domain, and HA2, which holds the fusion peptide (Figure 1). These subunits are linked by disulphide bonds [39]. Upon cleavage by host proteases, HA0 matures into the functional HA1-HA2 complex, forming two distinct domains: the stalk domain, primarily composed of HA2 with some HA1 residues, and the globular domain, or "head," primarily composed of HA1, which contains the SA binding pocket necessary for viral attachment, known as the receptor binding site (RBS) [31,40,41].

Mutations in the region near the RBS can significantly impact host specificity, as observed in the structural and amino acid differences between human- and avian-adapted strains [8–10,42]. In avian-adapted strains, HA recognizes and binds to α(2,3)-linked SAs, primarily found in the epithelial cells of the avian intestine. In contrast, human-adapted strains recognize α(2,6)-linked SAs, which are located in the upper respiratory tract of humans. These mutations that influence host specificity arise from two key processes: antigenic shift and antigenic drift.

Antigenic shift refers to abrupt, major changes in the viral genome, often resulting in a "species jump" through gene reassortment, as observed in the 2009 H1N1 swine flu pandemic [43,44]. Antigenic drift refers to an accumulation of gradual changes, resulting from direct infection followed by adaptation. Over time, natural selection favours mutations that enhance compatibility with the host species, as is commonly seen with avian viruses adapting to humans and contributing to seasonal flu epidemics [31,44].

While antigenic shift is responsible for enabling influenza viruses to cross species barriers, antigenic drift is crucial for sustaining efficient human-to-human transmission. This process is driven by the error-prone nature of viral polymerase and the selective pressures within the host environment [11,38,45]. The continuous genetic evolution through antigenic drift not only allows the virus to evade immune defences but also ensures its adaptation to the human population, ultimately supporting the spread of the virus beyond isolated spillover events. Therefore, to assess whether avian strains pose a potential pandemic threat to humans and to develop effective therapeutic interventions, it is crucial to investigate the mutations actively occurring in high-risk strains. These mutations hold the key to understanding the virus's ability to adapt and spread within human populations, and their identification is essential for guiding preventive measures and treatment strategies.

Figure 1 | HA structure of an Influenza A virus. 1) HA is a trimeric glycoprotein consisting of two domains: globular and stalk. 2a) HA consists of two domains: HA1 (orange) and HA2 (blue). HA1 primarily forms the globular head and contains the receptor-binding site (RBS) (yellow). 2b) The five antigenic sites of H3 HA subtype (A-E). [31,40]

Given the critical role of mutations, particularly those in close proximity to the RBS, continuous genetic and structural surveillance is vital. Monitoring these changes not only tracks the evolution of avian influenza viruses but also provides valuable insights into their potential for human-to-human transmission and pandemic risk. This makes the detailed study of amino acid-level mutations in the HA protein essential for understanding the threat posed by specific avian strains and for developing preventive measures and treatment strategies.

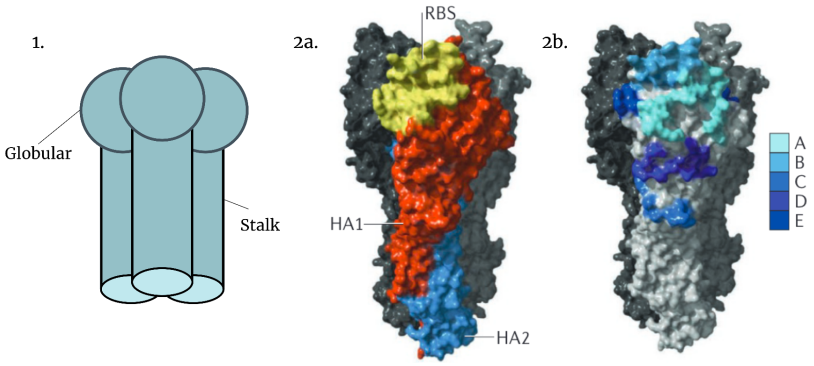

1.3 Leveraging Machine Learning in Predicting Glycan-Specificity

Historically, methods such as structural modelling, molecular docking, and glycan array assays have been widely used to predict glycan specificity [46–51]. These techniques have provided valuable insights into how mutations in HA influence viral binding to host receptors. However, these methods can be resource-intensive and less scalable when dealing with large datasets or rapidly evolving viral strains. Given the complexity of mutations, particularly near the RBS, traditional methods of genetic and structural analysis can be time-consuming and limited in scope.

Leveraging machine learning algorithms in this context offers a promising avenue for enhancing our ability to predict glycan-specificity in avian influenza viruses. In recent years, machine learning has proven to be a valuable complement to classical methods for predicting glycan specificity [13–19]. Machine learning enables the efficient analysis of large datasets, offering a scalable and dynamic approach to predicting viral behaviour with greater precision. Recent advancements in high-throughput sequencing (HTS) have provided vast viral sequence datasets, which, when integrated with machine learning models, enhance the detection of patterns and prediction of glycan interactions [52,53]. These HTS-generated datasets are essential in identifying key mutations in viral glycoproteins, such as HA, improving the understanding of viral adaptation and zoonotic potential. ML algorithms further enhance this process by continuously refining their predictions as new data becomes available, supporting the identification of mutations that may increase cross-species transmission and aiding in the anticipation of evolutionary changes that could pose future pandemic risks.

However, it is important to note that different prediction tasks require distinct algorithms, each designed to address specific facets of the problem. This diversity is especially pronounced when working with complex data, such as amino acid mutations in protein sequences, where different algorithms may vary in their effectiveness. Therefore, evaluating which machine learning algorithms are most appropriate for predicting glycan specificity from amino acid sequences of the HA protein is essential. Selecting the most effective models for this task can enhance the reliability and relevance of the generated predictions, ultimately improving the understanding of glycan interactions and their implications for viral behaviour.

1.4 Research Focus

This study hypothesises that machine learning algorithms can predict the glycan specificity of avian influenza viruses utilising publicly available viral sequence data, with varying degrees of accuracy. The aims of this research are two-fold: first, to leverage different machine learning methods to assess their performance in this prediction task and identify the most suitable algorithm; and second, to predict viral adaptations while pinpointing key genetic features that drive binding preferences by decoding the significance of these genetic features. Successful outcomes will enhance early detection of viral adaptations, improve risk assessments for human transmission, and support the development of targeted interventions for managing zoonotic outbreaks.

2. Materials & Methods

This section details the datasets, machine learning algorithms, and analytical methods employed to predict glycan specificity in the hemagglutinin protein of the influenza A virus. Glycan specificity is measured based on amino acid mutations that have been strongly correlated with enhanced viral binding to α(2,6) glycans, as identified in prior research [42,54–64]. To ensure consistency in analysis, the numbering scheme from Burke and Smith is utilised across the H3, H5, and H7 subtypes, allowing for effective comparison of mutations among these subtypes [65] .

The study leverages publicly available viral sequence data and implements several machine learning techniques using Python in the Google Colab environment to assess their predictive accuracy. The following subsections describe the key steps involved, including (1) dataset formation, (2) feature engineering, (3) model construction & prediction and (4) evaluation (Figure 2).

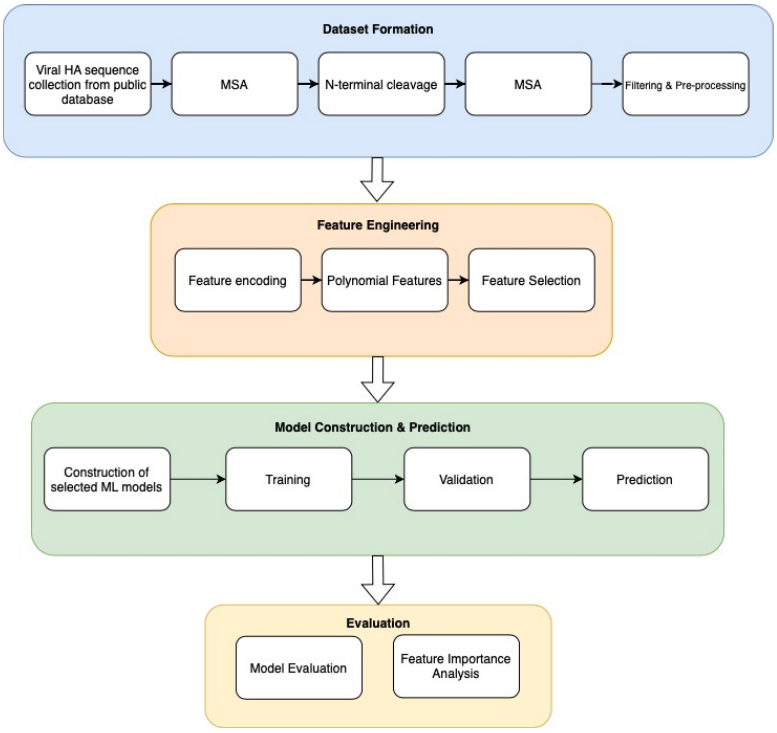
Dataset Formation
Viral HA sequence collection from public database
MSA
N-terminal cleavage
MSA
Filtering & Pre-processing
Feature Engineering
Feature encoding
Polynomial Features
Feature Selection
Model Construction & Prediction
Construction of selected ML models
Training
Validation
Prediction
Evaluation
Model Evaluation
Feature Importance Analysis

Figure 2 | Schematic representation of the machine learning pipeline used in this study.

2.1 Dataset Formation

In this section, key Python libraries such as NumPy, Pandas, and BioPython were used for numerical operations, data handling, and biological sequence processing, respectively. These libraries were central to the analyses performed in this part of the study.

2.1.1 Sequence collection from public database

Data from the 1900s onwards was sourced from GISAID's EpiFlu database (Figure 3), focusing on HA protein sequences of the H3, H5, and H7 subtypes. A total of 17,106 initial sequences from both human and avian hosts were collected in FASTA format for analysis.

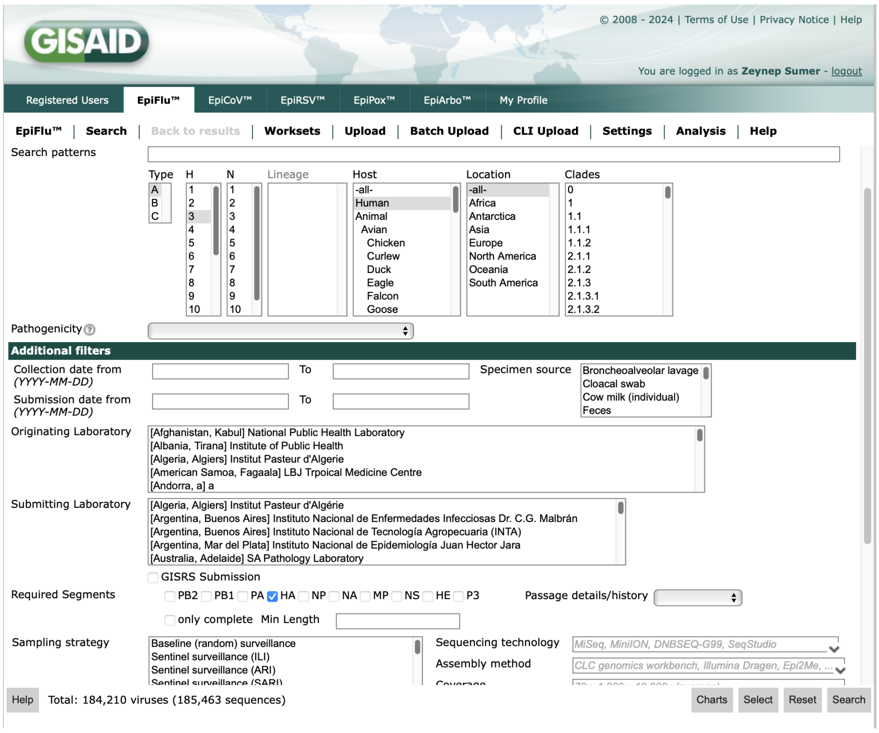
GISAID
© 2008 - 2024 | Terms of Use | Privacy Notice | Help
You are logged in as Zeynep Sumer - logout
Registered Users
EpiFlu™
EpiCoV™
EpiRSV™
EpiPox™
EpiArbo™
My Profile
EpiFlu™ | Search | Back to results | Worksets | Upload | Batch Upload | CLI Upload | Settings | Analysis | Help
Help
Charts
Select
Reset
Search

Search patterns

Type	H	N	Lineage	Host	Location	Clades
A	1	1		-all-	-all-	0
B	2	2		Human	Africa	1
C	3	3		Animal	Antarctica	1.1
	4	4		Avian	Asia	1.1.1
	5	5		Chicken	Europe	1.1.2
	6	6		Curlew	North America	2.1.1
	7	7		Duck	Oceania	2.1.2
	8	8		Eagle	South America	2.1.3
	9	9		Falcon		2.1.3.1
	10	10		Goose		2.1.3.2

Pathogenicity

Additional filters

Collection date from *(YYYY-MM-DD)* To

Submission date from *(YYYY-MM-DD)* To

Specimen source: Broncheoalveolar lavage, Cloacal swab, Cow milk (individual), Feces

Originating Laboratory:
[Afghanistan, Kabul] National Public Health Laboratory
[Albania, Tirana] Institute of Public Health
[Algeria, Algiers] Institut Pasteur d'Algerie
[American Samoa, Fagaala] LBJ Trpoical Medicine Centre
[Andorra, a] a

Submitting Laboratory:
[Algeria, Algiers] Institut Pasteur d'Algérie
[Argentina, Buenos Aires] Instituto Nacional de Enfermedades Infecciosas Dr. C.G. Malbrán
[Argentina, Buenos Aires] Instituto Nacional de Tecnología Agropecuaria (INTA)
[Argentina, Mar del Plata] Instituto Nacional de Epidemiología Juan Hector Jara
[Australia, Adelaide] SA Pathology Laboratory

□ GISRS Submission

Required Segments □ PB2 □ PB1 □ PA ☑ HA □ NP □ NA □ MP □ NS □ HE □ P3   Passage details/history

□ only complete Min Length

Sampling strategy: Baseline (random) surveillance, Sentinel surveillance (ILI), Sentinel surveillance (ARI), Sentinel surveillance (SARI)

Sequencing technology: *MiSeq, MinilON, DNBSEQ-G99, SeqStudio*

Assembly method: *CLC genomics workbench, Illumina Dragen, Epi2Me, ...*

Coverage

Total: 184,210 viruses (185,463 sequences)

Figure 3 | GISAID's EpiFlu Search & Browse interface displaying the applied filters for Influenza A H3 HA sequences from human hosts.

2.1.2 Multiple Sequence Alignment

Multiple sequence alignment (MSA) is a widely used computational method for aligning biological sequences, enabling the identification of conserved regions, evolutionary relationships, and functionally important motifs across different strains or species [66,67]. In this project, MSA is critical for aligning the HA protein sequences of Influenza A H3, H5, and H7 subtypes from human and avian hosts, facilitating a comprehensive analysis of sequence variation and subtype-specific characteristics. Accurate MSA is essential, as any discrepancies in alignment can lead to erroneous conclusions in subsequent analyses, undermining the biological relevance of the findings.

For the MSA of these sequences, MUSCLE (Multiple Sequence Comparison by Log-Expectation) has been chosen as the alignment tool due to its strong reputation for efficiency and accuracy, especially with large datasets. This algorithm employs a progressive alignment strategy combined with iterative refinement steps to enhance the overall quality of the alignment [66,68–70].

For this analysis, separate alignments for H3, H5, and H7 subtypes were performed, while aligning human and avian strains together within each subtype. This approach allows for the comparison of intra-subtype variation between different hosts and captures conserved regions across hosts, which is essential for understanding host adaptation and cross-species transmission dynamics.

MUSCLE was configured with the parameters: '-diags', and '-sv'. The '-diags' option ensures faster alignment by focusing on high-similarity diagonal regions in the dynamic programming matrix, which is especially beneficial for closely related sequences [71]. The '-sv' option invokes diagonal optimization with vertical refinement, further improving the alignment of sequences by refining gaps [72]. These settings enable efficient alignment while maintaining high quality for large datasets.

2.1.3 N-terminal Cleavage & Realignment (MSA)

The cleavage of the N-terminal region of the HA protein is essential for its maturation, which significantly impacts the virus's pathogenicity [39,40]. This maturation step is also crucial for establishing a standardised numbering scheme, as proposed by Burke and Smith (2014), ensuring consistent application across various H subtypes.

To facilitate this process, SignalP 5.0 was employed to predict the cleavage site of signal peptides, enabling the precise removal of the N-terminal regions from the aligned sequences of H3, H5, and H7. This ensures consistency in the numbering schemes across these subtypes[73]. After this removal, the sequences were realigned using the same parameters from the initial MSA to preserve the integrity of the alignment process. This realignment was essential to accommodate any positional changes that might have occurred during the trimming process, ensuring that subsequent analyses, including conserved region identification and mutation comparison, remain biologically relevant and accurate across subtypes.

2.1.4 Filtering & Pre-processing

Incomplete sequences and identical sequences, identified on a subtype and host basis, were removed to minimise noise in the dataset and ensure data integrity. This allowed for a more accurate analysis by reducing redundancies. The aligned sequences were stored alongside relevant metadata, including host, sequence, year, and subtype information, ensuring that each sequence could be traced back to its specific biological and temporal context.

2.2 Feature Engineering

Feature engineering refers to transforming raw data into a structured format that improves the performance and predictive accuracy of ML models during training. This process includes selecting, modifying, or creating features that effectively capture the underlying patterns within the data, which is critical for achieving optimal model outcomes [74,75].

In this project, the principles of feature engineering have been directly applied to optimise the analysis of protein sequences. Specifically, (1) feature encoding has been employed to extract feature vertices from amino acid sequences, while (2) polynomial features have been utilised for co-occurrence analysis. Furthermore, (3) feature selection methods have been implemented to identify a subset of relevant features, ensuring that only the most informative variables contribute to the predictive models. The sklearn.preprocessing and sklearn.feature_selection libraries were used to accomplish these tasks.

2.2.1 Feature Encoding

In this study, mutations located in close proximity to the RBS of the hemagglutinin protein were selected as key features, using the numbering scheme established by Burke and Smith (2014) to ensure consistent identification across subtypes. These selected mutations, defined by their original and mutated amino acids along with specific index information (Table 1), were crucial for understanding their correlation with phenotypic changes such as loss of N-glycosylation, increased stability, and increased binding to α(2,6) glycans [65].

Original	Mutated	H3 Index	H5 Index	H7 Index	References
H	Y	110	103	100	58,62,76
S	N	126	121	116	61
S	P	128	123	118	63
S	A	137	133	127	64
A	V	138	134	128	59
G	R	143	139	132	63
I	T	155	151	144	54,62,77
N	D	158	154	147	58
T	A	160	156	151	58
N	K	186	182	177	56,63,78
D	G	187	183	178	55
E	G	190	186	181	55,78
T	I	192	188	183	64
K	R	193	189	184	61
Q	R or H	196	192	187	55,63
V	I	214	210	205	62
Q	L	226	222	217	42,56,78,79
S	N	227	223	218	55–57
G	S	228	224	219	42,56,60,63
P	S	239	235	230	62

Table 1 | Selected Mutations in Proximity to the Receptor-Binding Site (RBS) Based on the Burke & Smith Numbering Scheme[65]

To transform this mutation data into a ML compatible format, multiple hot encoding was applied, marking the presence or absence of mutations at the specified positions. This encoding process converted the raw sequence data into feature vectors, which were then utilised in machine learning models to analyse their influence on viral characteristics. By employing this strategy, the study aimed to draw deeper insights into the mutations' roles in altering viral specificity, particularly in relation to RBS functionality.

2.2.2 Polynomial Features

Identifying co-occurring mutations in proteins is crucial for understanding their combined effects on protein structure, function, and evolutionary dynamics. These co-occurring mutations can reveal synergistic interactions that impact how proteins fold, interact with other molecules, or evade immune responses, particularly in viral proteins like influenza HA [80,81]. In viral evolution, such mutations may promote immune escape, altered pathogenicity, or enhanced receptor binding, cumulatively enhancing antigenic drift [82]. Since mutations rarely act in isolation, understanding their collective impact through co-occurrence analysis is essential for tracking evolutionary changes and informing strategic interventions. This is especially important in cases of synergy, where the combined effect of two mutations in a double mutant exceeds what would be expected from their individual contributions alone [80,83].

Given the importance of these combined effects, understanding co-occurring mutations in the HA protein is vital for unravelling the dynamics behind glycan specificity, a critical factor in viral attachment and host infection. In this study, polynomial features were employed to incorporate the co-occurrence of mutations into predictive models, improving the ability to monitor how these mutations influence glycan binding and, ultimately, viral evolution.

The sklearn.preprocessing library was used to capture complex, non-linear interactions between features. A polynomial degree of 3 was chosen to model cubic interactions, enabling the model to account for interactions among three variables at a time. This choice represents a tradeoff, balancing the modelling of higher-order interactions while minimising the risk of an excessively large feature space and diminishing returns.

2.2.3 Feature Selection

Feature selection was performed to reduce overfitting, particularly with polynomial features of degree 3, and to retain only the most relevant features for the model. This process also enabled the exploration of more complex interactions without being overwhelmed by irrelevant features. To achieve this, sklearn.feature_selection's SelectFpr function was applied, using the f_classif scoring function. The SelectFpr method performs univariate feature selection based on p-values derived from an ANOVA F-test, allowing for the retention of features that are most statistically significant[84]. An alpha value of 0.05 was used as the threshold, meaning features with a p-value less than 0.05 were kept for further analysis. This approach ensured a balance between reducing the feature space and preserving meaningful interactions, optimising model performance while maintaining interpretability.

2.3 Model Construction and Prediction

The classification task aimed to predict glycan specificity of HA protein sequences, where the features consisted of encoded amino acid sequences, and the labels indicated glycan binding (0 for avian binding and 1 for human binding). The objective was to determine which model would best predict glycan specificity based on known mutations in HA, as well as to identify the most significant features contributing to the prediction.

The selected models were trained and validated using GridSearch to identify the best estimator for each model, based on a range of relevant hyperparameters [85–87]. GridSearch performs training and validation simultaneously by partitioning the training set into multiple subsets, allowing for cross-validation [88]. This approach ensures that each model is evaluated on different portions of the data, removing the need for a separate validation set. The training data consisted of the H3, H5 and H7 dataset, while the remaining sequences from the H5 and H7 datasets were reserved as the test set for final model evaluation.

The classification models tested, in order of increasing complexity, were (1) Logistic Regression, (2) Support Vector Classifier (SVC) with a Linear Kernel, (3) Random Forest, and (4) XGBoost.

2.3.1 Construction of Selected Models

2.3.1.1 Logistic Regression

Logistic regression predicts the probability of a binary outcome (e.g., human vs. avian binding) based on one or more predictor variables (e.g., mutations in amino acid sequences). It models the log-odds of the outcome as a linear combination of the variables, expressed as:

$$Logit(P) \ = \ log\left(\frac{P}{1-P}\right) = \beta_0 + \beta_1 X_1 + \beta_2 X_2 + \ldots + \beta_n X_n \qquad (1)$$

where P is the probability of the outcome, $X_1, \ X_2, \ \ldots \ , X_n$ are the predictor variables, and $\beta_0, \beta_1, \ldots \ , \beta_n$ are the corresponding coefficients. The logistic function then converts the log-odds into probabilities for class prediction:

$$P(Y \ = \ 1 \,|\, X) \ = \ \frac{1}{1 + e^{-(\beta_0+\beta_1 X_1+\beta_2 X_2+\ldots+\ \beta_n X_n)}} \qquad (2)$$

This formulation allows for the identification of the most important mutations driving the outcome, making logistic regression useful for binary classification tasks in biological data[89,90].

In this study, logistic regression is used to predict glycan specificity of amino acid sequences. The model was implemented using scikit-learn's LogisticRegression. The model was fine-tuned using key hyperparameters for logistic regression, including regularisation strength (C), penalty function, and optimization solver, to enhance its ability to predict glycan specificity based on mutations[84].

2.3.1.2 SVC with Linear Kernel

SVC (Support Vector Classification) is a specific implementation of the broader Support Vector Machine (SVM) algorithm, designed for binary classification tasks. When using SVC with a linear kernel, the model aims to find the optimal hyperplane that maximises the margin between the two classes (e.g., human vs. avian glycan specificity)[91–93]. The equation of the hyperplane in n-dimensional space is given by:

$$w \cdot x + b = 0 \tag{3}$$

where w is the weight vector that defines the direction of the hyperplane, x is the input feature vector, and b is the bias term that adjusts the hyperplane position. The optimal hyperplane lies in the middle of this margin, ensuring the best possible class separation. The margin γ can be defined as:

$$\gamma = \frac{2}{||w||} \tag{4}$$

This margin is maximised by minimising the objective function:

$$min\frac{1}{2}\,||w||^2 \text{ subject to } y_i(w\,\cdot\,x_i+b)\;\geq\;1 \tag{5}$$

where y_i is the label of the data point x_i (either +1 or -1 for the two classes)[91–93] (see Figure 4).

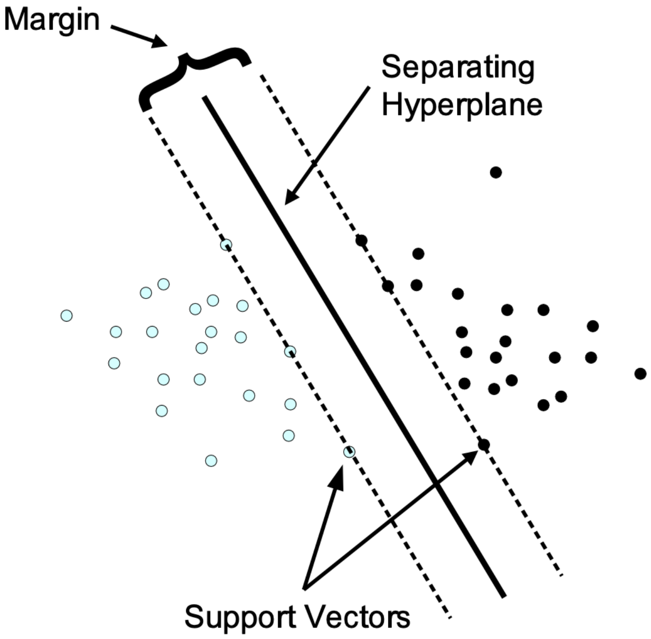

Figure 4 | Class separation in SVC with a linear kernel [92]

The SVC model was applied in this study to classify glycan specificity from encoded amino acid sequences, computing a linear separation between human and avian classes. The SVC function from sklearn.svm was implemented with a linear kernel with a class weight balancer to address potential class imbalance. Key parameters such as the C parameter , tol (tolerance for stopping criteria) were tuned to improve regularisation and convergence, enhancing accuracy and generalisation in glycan specificity prediction.

2.3.1.3 Random Forest

Random Forest is an ensemble learning algorithm that combines multiple de-correlated decision trees to improve prediction accuracy. Each tree is trained on a randomly sampled subset of the data, helping the model avoid overfitting and handle both quantitative and qualitative input variables. This approach is particularly effective for large datasets and can manage redundant or highly correlated features, leading to robust classification results [94,95].

Random Forest efficiently handles high-dimensionality by building multiple decision trees that capture interactions between features (Figure 5). This reduces the risk of overfitting while improving generalisation, making it ideal for predicting glycan binding based on encoded mutation data. In Random Forest, multiple decision trees are constructed through a process called bagging, where each tree classifies an input x into a class C based on the majority vote:

$$\hat{y} = mode(\{T_1(x), T_2(x), \ldots, T_n(x)\}) \tag{6}$$

where $T_1(x), T_2(x), \ldots, T_n(x)$ represent the predictions made by each individual tree. The mode function finds the most frequent value (class) among the predictions made by the individual trees $T_1, T_2, \ldots, T_n$. The class that appears most often is considered the final prediction ($\hat{y}$)[96].

The Random Forest model was employed in this study to predict glycan specificity based on encoded mutation data, leveraging its ability to handle high-dimensionality through ensemble learning. The RandomForestClassifier from sklearn.ensemble was used, with key hyperparameters such as the number of estimators (trees), maximum depth of each tree, the minimum number of samples required to split an internal node, and the minimum number of samples required to be at a leaf node being fine-tuned to balance model complexity and overfitting.

Figure 5 | Visualisation of the random forest algorithm[94]

2.3.1.4 XGBoost

XGBoost (Extreme Gradient Boosting) is a scalable ML algorithm based on tree boosting, which integrates multiple decision trees to improve prediction accuracy. It uses second-order Taylor expansion for optimization and is known for handling large datasets efficiently through parallel computing.

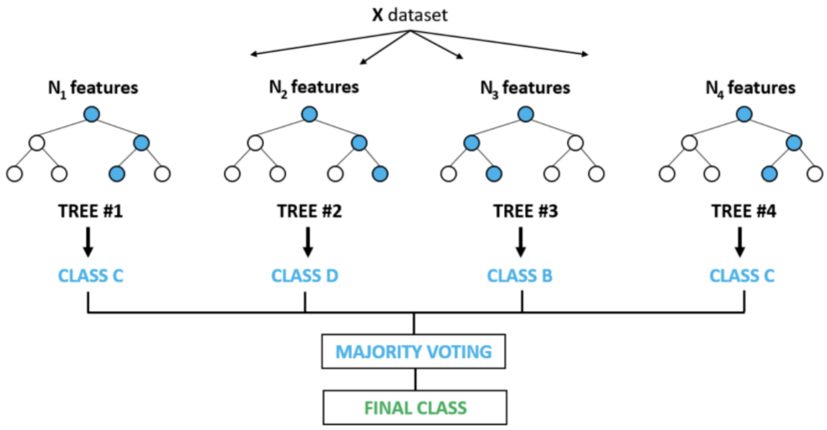

XGBoost employs a series of decision trees for prediction, where each tree contributes to refining the overall model output. The prediction for an instance is represented as the sum of the outputs from all trees, expressed mathematically as:

$$\hat{y} = \sum_{k=1}^{K} f_k(x) \tag{7}$$

where $\hat{y}$ is the predicted value, K is the number of trees, and $f_k(x)$ is the output of the k-th tree for the input features x[97].

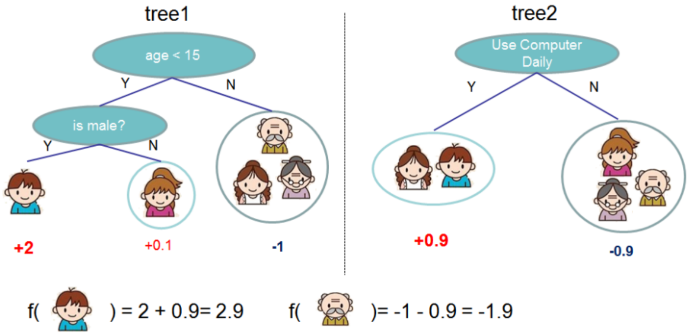

Figure 6 | XGBoost tree ensemble model.[97]

XGBoost prevents overfitting by incorporating regularisation techniques and shrinkage, making it well-suited for binary classification tasks. When applied to complex data such as multiple one-hot encoded amino acid sequences for predicting glycan specificity, XGBoost's ability to handle large, high-dimensional datasets and complex feature interactions ensures robust performance [97,98].

In this project, the XGBClassifier from the xgboost library is used with a grid detailing key hyperparameters such as the number of estimators, tree depth, learning rate, minimum loss reduction needed for splits (gamma) and booster.

2.3.2 Training & Validation

The training and validation process uses GridSearchCV from sklearn.model_selection with a 5-fold cross-validation approach. GridSearchCV searches the hyperparameter grid to find the best hyperparameter combination, optimising the weighted F1 score to balance precision and recall. This ensures the best estimator is selected for the classification task, leading to a more reliable model.

2.3.3 Prediction

In the prediction stage, once the best estimator was selected through GridSearchCV using 5-fold cross-validation, predictions were made on the test set, which consisted of H5 and H7 data. These test sets were distinct from the training set, allowing for an unbiased evaluation of the model's performance on unseen data. The results of the predictions were evaluated using the methods outlined in section 2.4, ensuring a comprehensive assessment of accuracy, precision, recall, and other relevant metrics for the binary classification task.

2.4 Evaluation

Evaluating ML models is a crucial step to ensure their robustness and suitability for specific tasks. Common evaluation methods include validation, classification report, and feature importance analysis.

Validation analysis involves analysing techniques such as cross-validation, which helps in assessing how the results of a statistical analysis will generalise to an independent dataset. This method splits the data into several subsets, or folds, where the model is trained on a portion of the data and tested on the remaining subset. By averaging the performance metrics across all folds, validation analysis provides a more reliable estimate of the model's predictive performance and helps mitigate issues related to overfitting.

The classification report provides insights into precision, recall, and F1-scores for each class, giving a detailed view of a model's performance, based on four fundamental outcomes: true positives (TP), true negatives (TN), false positives (FP), and false negatives (FN). These metrics collectively offer a comprehensive evaluation of the model's effectiveness in classifying the positive and negative classes, ensuring a deeper understanding of its strengths and weaknesses.

Feature importance analysis, on the other hand, aims to identify which features significantly influence the model's predictions. Techniques such as permutation importance or tree-based methods (like those used in Random Forest and XGBoost) rank features based on their contribution to the model's accuracy. Understanding feature importance is essential for interpreting the model and can guide further feature selection, ensuring that the model relies on the most relevant data, ultimately leading to improved performance and insights into the underlying processes being modelled

3. Results

3.1 Model Evaluation

3.1.1 Data Overview

To facilitate a clear understanding of the subsequent analysis and discussion, it is essential to first examine the dataset itself. The dataset comprises multi-hot encoded arrays, where each feature is binary (0 or 1), representing the presence or absence of specific categories (mutations). These categories capture different attributes or characteristics relevant to the problem under study, and the target variable is binary, indicating two possible outcomes (e.g., avian or human binding). Prior to filtering and preprocessing, the dataset initially contained 17,106 sequences, but after removing identical and incomplete sequences, this was reduced to 8,579 sequences.

To evaluate subtypes that have not yet established themselves in human hosts, 100% of the H3 dataset—an established subtype in both human and avian hosts—was allocated for training, providing a robust foundation. In contrast, only 20% of the H5 and H7 datasets were reserved for training, with the remaining 80% designated for testing. The H3 strain's extensive documentation in both human and avian hosts allowed for a larger number of available sequences compared to the predominantly avian H5 and H7 strains, which resulted in class imbalance. To mitigate this imbalance, SMOTE was applied to synthetically increase the representation of H5 and H7 sequences, with a specific focus on augmenting human samples. This process ensured a more balanced dataset for model training. After applying SMOTE, the total number of sequences increased to 9,964 (see Figure 7). However, a slight imbalance still persisted in the H3 dataset between human and avian hosts, which will be taken into account during the following stages of analysis.

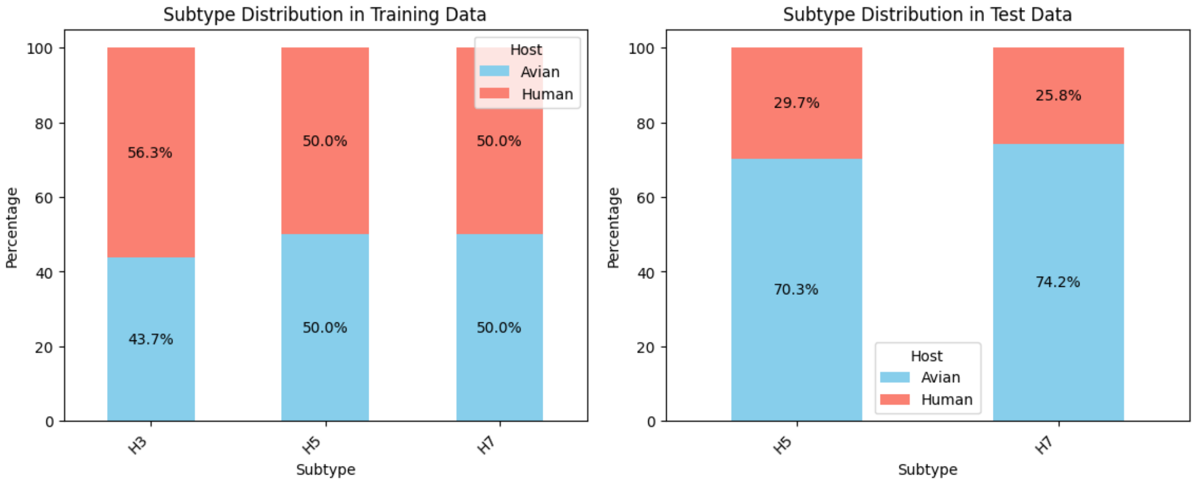

Figure 7 | Avian and human host ratios of the (a) training and (b) testing data sets.

3.1.2 Validation Results

In this study, GridSearchCV was employed to optimise each model by identifying the best-performing estimator based on validation results, prior to testing on unseen data. A 5-fold cross-validation ensured balanced representation of both avian and human samples in each fold, minimising bias and providing a robust evaluation of model performance.[87,99,100].

The F1-weighted score was selected as the primary metric during this process, representing a weighted average of the F1 scores for each class, with weights proportional to the number of true instances (support). This metric is particularly useful for imbalanced datasets, as it accounts for performance across both majority and minority classes, preventing dominance by the majority class.

The formula for calculating the F1 score for each class is:

$$F1 = \frac{2 \times Precision \times Recall}{Precision + Recall} \quad (8)$$

Where precision is the ratio of true positives to the sum of true positives and false positives (as shown in Equation (9)) [101–103]

$$Precision = \frac{TP}{TP + FP} \quad (9)$$

and recall is the ratio of true positives to the sum of true positives and false negatives (as shown in Equation (10)) [101–103]

$$Recall = \frac{TP}{TP + FN} \quad (10)$$

The F1-weighted score helps evaluate the model's performance during cross-validation, balancing precision and recall across both classes. It ensures that the model is not biassed toward the majority class, providing a more accurate assessment of its generalisation ability. After cross-validation, hyperparameters are selected based on the configuration yielding the best validation score, which indicates how well the model generalises to unseen data. A high validation score suggests effective learning of generalizable patterns, while a significant drop from training performance may indicate issues like overfitting or poor generalisation, particularly in imbalanced datasets [99,100]. By analysing the validation scores, one can assess the robustness of the model and its ability to adapt to variations in real-world data.

In Table 2, the best weighted F1-scores for each classification algorithm are presented. Logistic Regression achieves the highest score at 0.534, indicating a balanced performance between precision and recall across classes. Following closely, Random Forest and XGBoost score 0.506 and 0.521, respectively, demonstrating their effectiveness in handling the classification task, albeit slightly less than Logistic Regression. SVC with a Linear Kernel has the lowest score at 0.442, suggesting challenges in generalising unseen data compared to the other models. These scores provide valuable insights into the relative strengths and weaknesses of each algorithm for this particular classification problem.

Classification Algorithm	**Best Weighted F1-Score**
Logistic Regression	0.534
SVC with Linear Kernel	0.442
Random Forest	0.506
XGBoost	0.521

Table 2 | Cross Validation Results of Selected ML Methods

3.1.3 Classification Report

Analysing the classification report is crucial for understanding the performance of models in classification tasks. Accuracy, one of the key metrics reported, is defined as the proportion of true positive and true negative predictions among the total predictions made. It is calculated using the formula:

$$Accuracy = \frac{TP + TN}{TP + TN + FP + FN} \tag{11}$$

When interpreting accuracy, it's important to consider the context of the dataset, especially in cases of class imbalance, as high accuracy might be misleading if the model predominantly predicts the majority class.Table 3 summarises the classification results of all the models used, illustrating their varying strengths in precision, recall, F1-score, and accuracy. The classification results highlight the challenges presented by the imbalance in the dataset, primarily due to the significantly greater number of avian samples for H5 and H7. This highlights the importance of choosing a model that can effectively handle these imbalances while delivering robust predictions. The ultimate goal is to identify a model that not only performs well overall but also ensures reliable classification of the minority class.

Classifier	**Precision**	**Precision (Weighted)**	**Recall**	**Recall (Weighted)**	**F1-Score**	**F1-Score (Weighted)**	**Accuracy**
Logistic Regression	0.726 (0), 0.000 (1),	0.528	1.000 (0), 0.000 (1)	0.726	0.842 (0), 0.000 (1)	0.611	0.726
SVC with Linear Kernel	0.727 (0), 1.000 (1)	0.802	1.000 (0), 0.004 (1)	0.728	0.842 (0), 0.008 (1)	0.614	0.728
Random Forest	0.730 (0), 1.000 (1)	0.804	1.000 (0), 0.017 (1)	0.731	0.844 (0), 0.033 (1)	0.622	0.731
XGBoost	0.711 (0), 0.000 (1)	0.505	1.000 (0), 0.000 (1)	0.711	0.831 (0), 0.000 (1)	0.591	0.711

Table 3 | Cross Validation Results of Selected ML Methods

Among the models evaluated, Random Forest stands out as the most effective for prediction, achieving the highest accuracy (0.731) and weighted F1 score (0.622) , demonstrating a better balance between precision and recall compared to its counterparts. It effectively addresses the challenges associated with the minority class that both Logistic Regression and XGBoost encounter, as both models exhibit low recall for class 1, indicating their failure to identify critical instances of this class. Although the SVC with Linear Kernel achieves perfect precision for class 1, it struggles to accurately identify the majority class, as evidenced by its low F1-score. This highlights the importance of evaluating overall performance across both classes, rather than solely focusing on precision or recall for one class. Therefore, while Random Forest leads in accuracy and overall performance, a careful evaluation of each metric is essential to select a model that effectively addresses the specific needs of this classification task, particularly in the context of mitigating the effects of data imbalance in the test set.

3.2 Feature Interpretation

Feature interpretation is essential in understanding how different variables contribute to model predictions, and in some cases, improving predictive performance[104]. This process deepens understanding of the domain and supports informed decision-making. In the context of identifying significant mutations that influence glycan specificity classification, feature interpretation helps pinpoint the mutations with the greatest impact on glycan specificity determination. Each mutation is represented as a feature in the model, and the magnitude of its coefficient indicates its influence on the classification outcome.

The approach to feature interpretation varies between linear models and tree-based models. In linear models, such as Logistic Regression and Linear SVC, feature weights are directly represented by the model coefficients. These coefficients (β) reflect the strength and direction of the relationship between each feature (x) and the target variable (y), enabling straightforward interpretation.

The relationship can be mathematically expressed as:

$$y = \beta_0 + \beta_1 x_1 + \beta_2 x_2 + \ldots + \beta_n x_n \tag{12}$$

When evaluating feature importance in linear models, features should be ranked based on the absolute values of these coefficients (|β|). This ranking allows for an understanding of the influence of each feature on the target variable, irrespective of the direction of the relationship. A larger absolute value indicates a stronger influence on y.

In contrast, tree-based models, such as Random Forest and XGBoost, use metrics like Gini impurity or information gain (based on entropy) to assess feature importance [96,97]. These metrics evaluate how well a feature splits the data into more homogeneous subsets, assigning importance scores based on the total reduction in impurity achieved across all trees in the model. A higher importance score indicates a stronger influence on the model's predictions, but unlike linear models, these scores do not indicate whether the feature has a positive or negative impact on the target—only its overall contribution to improving the model's accuracy. Features that lead to larger decreases in impurity have a more significant impact on the model's classification performance.

To interpret feature importance effectively across all models, the absolute value of the linear models' coefficients is first taken to focus on their magnitude, as the sign (positive or negative) in linear models shows the direction of the relationship, not its importance. Next, all coefficients and feature importance scores are normalised to compare features across different models. This ensures that each feature’s relative importance is evaluated within its own model, independent of scale. The normalised importance for each feature I_{f_i} can be calculated using the formula:

$$I_{f_i} = \frac{|w_i|}{\sum_{i=1}^{n} \quad |w_i|}$$

(13)

Where $|w_i|$ is the absolute value of the linear model coefficient or the raw feature importance from a tree-based model, and n is the total number of features. This normalisation allows for a fair comparison across both linear and tree-based models, highlighting the most impactful features in each.

Figure 7 shows the normalised feature importances across four machine learning models: Logistic Regression, SVC with Linear Kernel, Random Forest, and XGBoost, using mature H3 indices. The plot effectively compares the relative importance of features across these models, with normalisation ensuring that each feature's importance is evaluated within its own model, independent of scale. This allows for fair comparison across models despite their different mechanisms for determining feature importance.

For the linear models (Logistic Regression and SVC with Linear Kernel), feature coefficients were first converted to absolute values, removing the sign to focus solely on the magnitude of the feature's influence. This approach ensures that only the strength of the relationship is considered, not whether it's positive or negative. In the tree-based models (Random Forest and XGBoost), raw feature importance scores—based on impurity reduction—were used directly.

The features with higher bars in the plot contribute more significantly to the model's performance. Three main mutations—Tto_I_at_192, S_to_N_at_227, and Q_to_L_at_226—along with their polynomial variants, stand out as the most influential features across different models. These mutations significantly impact the predictions, highlighting their biological relevance and suggesting that they play crucial roles in the underlying mechanisms being modelled. The variations in their importance, especially when considering both base and polynomial features, provide valuable insights into how these mutations may interact with other factors and influence the overall model behaviour.

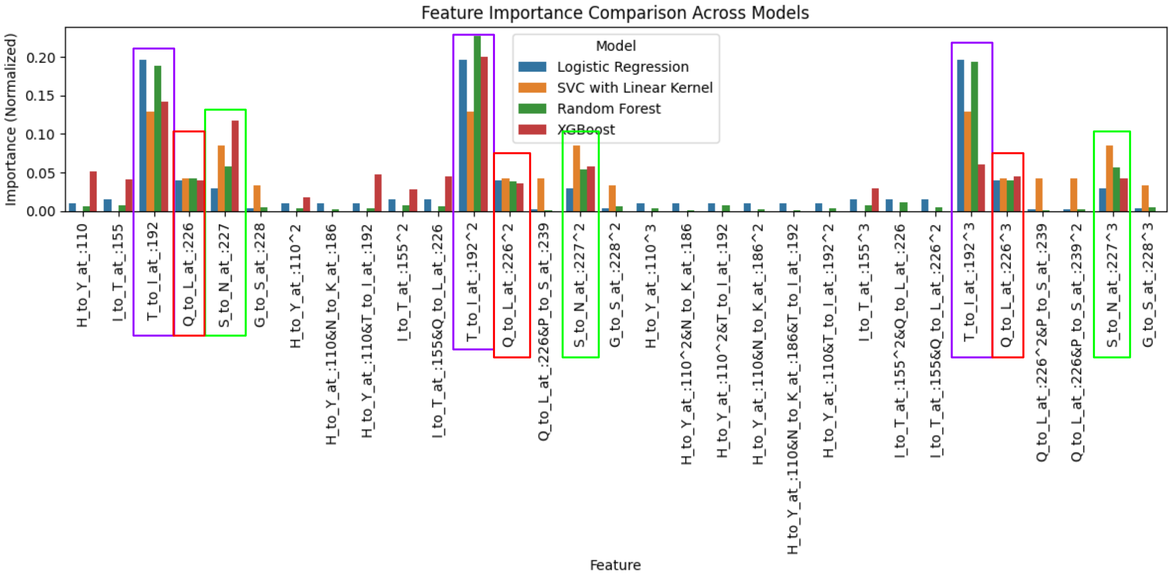

Figure 8 | Feature Importance Comparison Across Models

T_to_I_at_192 stands out as a significant feature, with both the base mutation and its polynomial variants displaying consistently high importance across the different models. This suggests that the threonine (T) to isoleucine (I) substitution at position 192 in mature H3 plays a pivotal role in predicting the outcome. The persistence of importance in the higher-order features, such as T_to_I_at_192^2 and other polynomial variants, implies that this mutation does not solely exhibit a simple linear relationship with the target variable. Instead, its influence appears to extend into more complex, non-linear domains, where interactions between this mutation and other features become relevant. The higher-degree polynomial terms likely capture these nuanced interactions or effects that the linear feature alone cannot fully explain. This could reflect intricate biological mechanisms, such as structural changes in the protein that are influenced by multiple factors simultaneously, which lead to non-linear contributions to the model's predictions. Therefore, the importance of these polynomial terms suggests a deeper, layered impact of the T_to_I_at_192 mutation, making it a critical feature for the models' performance.

The feature S_to_N_at_227 and its polynomial variants (e.g., S_to_N_at_227^2) also show varying levels of importance across the models. The base mutation, S_to_N_at_227, represents a point mutation where serine (S) is replaced by asparagine (N) at position 227 in the protein sequence. This feature likely has biological significance, suggesting that changes at this specific position might have notable effects on the protein's structure or function. However, as the polynomial variants (e.g., S_to_N_at_227^2) are introduced, their importance tends to decrease across the models. This decline in importance suggests that while the base mutation at position 227 is crucial, the mutation has a more direct, linear effect on the outcome, with limited non-linear interactions or higher-order contributions.

In addition to T_to_I_at_192 and S_to_N_at_227, the mutation Q_to_L_at_226 also warrants attention. This mutation involves the substitution of glutamine (Q) with leucine (L) at position 226 in the mature H3 protein sequence. The importance of this mutation, as reflected in the models, indicates that it may play a significant role in the protein's functionality or stability. The Q_to_L_at_226 substitution may affect the protein's structure and interactions, as leucine is a hydrophobic amino acid, whereas glutamine is polar and capable of forming hydrogen bonds. This change could influence how the protein folds or interacts with other molecules, potentially altering its biological activity.

Analysing the polynomial variants of Q_to_L_at_226 reveals that there is little to no variation in their importance across the models. This suggests that the impact of this mutation is primarily captured by the base mutation itself, indicating that complex non-linear interactions may not significantly influence its contribution. Understanding the implications of Q_to_L_at_226, alongside T_to_I_at_192 and S_to_N_at_227, provides a comprehensive view of these mutations' roles in the model and their potential effects on the protein's function. This consistency underscores the straightforward relationship between the Q_to_L_at_226 mutation and the model's predictions.

4.Discussion

The findings of this study underscore the complexities and challenges of using machine learning algorithms to predict the glycan specificity of the HA protein in avian influenza viruses. While we successfully identified key genetic features and assessed various algorithms, several limitations arose due to data constraints and resource availability. This discussion will explore these limitations, highlight key findings related to model performance and significant mutations, and propose future research directions to enhance the predictive capabilities and understanding of viral behaviour.

4.1 Limitations

This study faces several limitations primarily related to data availability and time & resource constraints. First, the scarcity of human H5 and H7 sequences significantly affects the training and testing of machine learning models. Despite the application of oversampling techniques, such as synthetic data generation (SMOTE), the limited availability of real-world data reduces the models' reliability, as synthetic data may not fully capture the complexity and variability inherent in natural sequences. This directly impacts model performance and generalizability. Additionally, time and resource constraints played a role in limiting the depth of this research. The study was conducted over a span of six months, restricting the exploration of mathematical and structural analyses that could provide further insights into the model's results. Techniques such as PCA, permutation feature importance, and correlation analysis were not fully explored. Experimentation with hyperparameters was also limited due to the computational intensity of methods such as grid search. The computational cost of increasing the number of parameters was prohibitively high and as a result, the models used may not reflect their optimal configurations, potentially affecting predictive accuracy.

Lastly, the study's focus on the sequence of a single gene represents a reductionist approach, addressing only one element of the virus-host interaction. It is important to acknowledge that glycan binding is merely one part of the intricate infection process. Binding alone does not ensure successful infection, as other factors play critical roles in determining infection outcomes. Elements such as the host's immune response and viral replication efficiency also influence the overall infection dynamics. Incorporating these additional variables in future work would provide a more holistic understanding of the infection process. Expanding the model to account for a wider range of factors beyond glycan binding would improve its predictive capabilities and offer more comprehensive insights into viral behaviour.

4.2 Key Findings

4.2.1 Model Performance

The evaluation of various classification algorithms revealed distinct performance characteristics. Logistic Regression attained the highest weighted F1-score (0.534) when applied to a balanced validation set; however, it underperformed in classification metrics when assessed on the imbalanced test data. In contrast, the Random Forest algorithm demonstrated superior overall performance in classification reports, exhibiting robust accuracy and F1 scores, which indicate its enhanced capability to manage the imbalanced nature of the H5 and H7 data. Although simpler models may excel in identifying feature importance, ensemble methods such as Random Forest appear to be more effective for classification tasks, particularly in the context of challenging datasets.

The observed model performance disparities highlight the influence of an imbalanced test set. While SMOTE was applied to create balanced training and validation sets, the imbalanced nature of the test data led to challenges in accurately classifying instances of the minority class. As a result, models such as Random Forest, XGBoost, and SVC with a Linear Kernel performed less effectively on the test set, particularly in recalling the human-binding class. This situation emphasises that while SMOTE can enhance validation scores by mitigating class imbalance, the model's performance in real-world scenarios—represented by the test set—can still be adversely affected by imbalanced distributions. Therefore, to achieve reliable predictions, it is crucial to consider the distribution of the test set and tailor model evaluation strategies accordingly.

The integration of polynomial features, specifically the incorporation of co-occurrence among mutations, yielded some insightful observations, albeit not entirely as anticipated. For certain mutations, this approach elucidated the relationship between individual mutations and glycan specificity classifications. However, it did not reveal the expected co-occurrence among multiple distinct mutations. This limitation suggests that while the polynomial feature integration provided valuable insights, its potential remains underutilised in the current model framework. Future enhancements to the model may enable a more effective exploitation of this polynomial approach, allowing for a deeper understanding of the intricate relationships among mutations and their collective impact on glycan specificity.

4.2.2 Key Mutations

Through our machine learning pipeline, three key mutations emerged with the highest feature importance across all selected models: T192I (T_to_I_at_192), Q226L (Q_to_L_at_226), and S227N (S_to_N_at_227). These mutations reside in critical loops and helices of the protein, including the 130 loop, 190 helix, and 220 loop, as well as antigenic regions, which may significantly impact the overall structure and functional properties of the protein[105]. The molecular properties of the involved amino acids—such as polarity, hydrophobicity, and hydrogen bonding capabilities—are pivotal in determining the protein's stability and conformation. Alterations in these regions could lead to changes in glycan specificity by affecting the binding interactions between the protein and glycans. Understanding the implications of these mutations on the protein structure, glycan interactions, and immune recognition is crucial for elucidating their potential roles in viral pathogenesis and immune evasion.

4.2.2.1 T192I (T_to_I_at_192)

The T192I mutation significantly alters the 130 loop (indices 135-135) and the 190 helix, both of which are integral to the protein's structural integrity and functionality. This mutation has been confirmed in glycan microarray studies, indicating its role in glycan specificity. The original residue, threonine (T), is uncharged and polar, capable of forming hydrogen bonds, which is crucial for maintaining interactions within the protein structure. In contrast, the isoleucine (I) residue is hydrophobic and nonpolar, lacking hydrogen bond formation capabilities. This change can disrupt the loop's conformation, affecting how the protein interacts with glycans. Additionally, the T192I mutation is located in antigenic region B, highlighting its potential impact on immune recognition and antibody binding, as changes in this region can influence how effectively the immune system can target the protein.

4.2.2.2 Q226L (Q_to_L_at_226)

The Q226L mutation is particularly noteworthy due to its strong connections to glycan specificity as reported in the literature[42,56,78,79,105,106]. Positioned within the receptor-binding site, this mutation is crucial for interactions with glycan ligands. While it has commonly been observed to co-occur with G228S, this relationship was not captured in the current model. The substitution from glutamine (Q) to leucine (L) can significantly affect hydrogen bond formation and van der Waals interactions between the SA moiety and the protein[105]. The alteration in side-chain properties may modify the binding affinity and specificity for glycans. Additionally, Q226L resides in the 220 loop, a region known for allowing viral escape from broadly neutralising antibodies. Thus, changes in this loop could enhance the virus's ability to evade immune detection, further emphasising the significance of this mutation.

4.2.2.3 S227N (S_to_N_at_227)

The S227N mutation introduces an asparagine (N) residue in place of serine (S), which can influence the structural dynamics of the protein[79]. The presence of the polar, hydrophilic asparagine could affect local interactions within the protein, potentially altering the conformation of surrounding loops and helices. Given that this mutation is also situated in the vicinity of crucial binding sites, any structural changes could impact the protein's glycan specificity and its overall stability. While S227N may not be as well characterised in the literature as the previous mutations, its placement in a functional region suggests it could still play a role in the protein's interaction with glycans and its recognition by antibodies.

In summary, the integration of these mutations into key loops and helices and their positioning within antigenic sites underscores their significance in influencing the protein's structure, functionality, and interactions with glycans and the immune system. Understanding these relationships is vital for elucidating the underlying mechanisms of glycan specificity.

4.3 Future Works

4.3.1 Exploration of Therapeutic Applications

The identification of key mutations in the HA protein, particularly those influencing glycan specificity and antigenic properties, can significantly enhance vaccination efforts by deepening our understanding of viral evolution and immune evasion strategies [15,61,76]. Moreover, integrating predictive models to assess mutation-driven changes in antigenicity could refine antigen selection for seasonal vaccines, ultimately leading to more effective immune responses and reducing the need for frequent updates. This predictive insight would also facilitate the preventive development of broadly neutralising vaccines by identifying conserved regions in HA that are less prone to mutation, ensuring long-lasting immunity[107].

4.3.2 Improving the Predictive Model

To enhance the predictive model's accuracy and applicability in understanding HA protein mutations, several advanced deep learning techniques can be leveraged. Neural networks (NNs) are particularly effective at capturing the intricate patterns present in biological data, making them invaluable for predicting the antigenic properties and binding interactions of viral proteins. Deep neural networks, especially when integrated with protein language models such as ProtTrans, ESM-2, and ESM-1b, offer a significant advancement in feature representation. These models utilise vast datasets of protein sequences to generate embeddings that encapsulate essential biological features. By leveraging this rich contextual information, the predictive capabilities of the model are greatly enhanced, allowing for more accurate forecasts of how mutations may affect binding and immune recognition.

To refine the model's predictive power, it is also beneficial to expand the classification framework to a three-state classification system—non-binder, weak binder, and strong binder—based on biological assays. This nuanced approach allows for better differentiation among varying levels of binding affinity. For example, a strong binder may warrant a different vaccine formulation or dosing strategy than a weak binder. This refined approach ensures that vaccines are optimised for the specific antigenic properties of the targeted virus, potentially improving overall effectiveness.

Furthermore, the incorporation of structural information into the predictive framework can substantially enrich the analysis of binding sites. For example, examining the threedimensional structures of the HA protein (through sources such as the Protein Data Bank) and its interactions with immune components can provide critical insights into how specific mutations and spatial arrangements influence binding affinities. Such insights can lead to the identification of critical residues that govern interactions, thus refining the model's accuracy.

Lastly, applying this enhanced predictive model to other subtypes, such as H9, not only broadens the scope of the analysis but also helps generalise findings across different viral strains. Training the model on diverse datasets allows it to adapt to various antigenic landscapes, ultimately improving predictive accuracy for emerging strains. This adaptability is crucial for developing more effective and broadly applicable vaccination strategies, which can respond proactively to viral evolution and immune evasion tactics.

4.4 Conclusion

This study investigated the utility of machine learning algorithms in predicting the glycan specificity of the HA protein of the influenza A virus, hypothesising that varying degrees of accuracy could be achieved using viral sequence data. We achieved our objectives by employing various machine learning methods, evaluating their performance, and identifying the most suitable algorithm for this task. Additionally, we pinpointed key genetic features that drive binding preferences, enhancing our understanding of viral adaptations. While this research provides a foundational understanding, further improvements, as highlighted in the future works section, could enhance the predictive capability and applicability of these models.

Acknowledgements

I would like to thank my supervisor, David Burke, for their guidance and support throughout the course of this dissertation. His expertise has been invaluable to the development of this work.

I would also like to acknowledge the program leads, particularly David Moyes, for their leadership and the structure they provided to the Microbiome MSc course. His support has been greatly appreciated.

Finally, I am grateful to my classmates for their collaboration and shared insights during this journey.

Supplementary Material

The code utilised in this study has been included as supplementary material and is provided as a separate attachment. This supplementary file contains all relevant scripts and implementations necessary to reproduce the findings discussed in the main text.

References

1. Number of COVID-19 cases reported to WHO. *WHO COVID-19 dashboard* https://data.who.int/dashboards/covid19/cases?n=c. (2024).
2. Past pandemics. *World Health Organization* https://www.who.int/europe/news-room/fact-sheets/item/evaluation-of-the-response-to-pandemic-(h1n1)-2009-in-the-european-region#:~:text=2009%20pandemic&text=For%20the%20first%20time%2C%20pandemic,in%20the%20first%20year%20alone. (2010).
3. Chen, J. *et al.* Novel Reassortant Avian Influenza A(H5N6) Virus, China, 2021. *Emerg. Infect. Dis.* **28**, 1703–1707 (2022).
4. Focosi, D. & Maggi, F. Avian Influenza Virus A(H5Nx) and Prepandemic Candidate Vaccines: State of the Art. *Int. J. Mol. Sci.* **25**, 8550 (2024).
5. Naguib, M. M. *et al.* Global patterns of avian influenza A (H7): virus evolution and zoonotic threats. *FEMS Microbiol. Rev.* **43**, 608–621 (2019).
6. Oliver, I. *et al.* A case of avian influenza A(H5N1) in England, January 2022. *Eurosurveillance* **27**, (2022).
7. Shi, J., Zeng, X., Cui, P., Yan, C. & Chen, H. Alarming situation of emerging H5 and H7 avian influenza and effective control strategies. *Emerg. Microbes Infect.* **12**, 2155072 (2023).
8. Bradley, K. C. *et al.* Comparison of the receptor binding properties of contemporary swine isolates and early human pandemic H1N1 isolates (Novel 2009 H1N1). *Virology* **413**, 169–182 (2011).
9. Connor, R. J., Kawaoka, Y., Webster, R. G. & Paulson, J. C. Receptor Specificity in Human, Avian, and Equine H2 and H3 Influenza Virus Isolates. *Virology* **205**, 17–23 (1994).
10. Ibricevic, A. *et al.* Influenza Virus Receptor Specificity and Cell Tropism in Mouse and Human Airway Epithelial Cells. *J. Virol.* **80**, 7469–7480 (2006).
11. Long, J. S., Mistry, B., Haslam, S. M. & Barclay, W. S. Host and viral determinants of influenza A virus species specificity. *Nat. Rev. Microbiol.* **17**, 67–81 (2019).
12. Raman, R., Tharakaraman, K., Sasisekharan, V. & Sasisekharan, R. Glycan–protein interactions in viral pathogenesis. *Curr. Opin. Struct. Biol.* **40**, 153–162 (2016).
13. Garjani, A. *et al.* Forecasting influenza hemagglutinin mutations through the lens of anomaly detection. *Sci. Rep.* **13**, 14944 (2023).
14. Xu, Y. & Wojtczak, D. Dive into machine learning algorithms for influenza virus host prediction with hemagglutinin sequences. *Biosystems* **220**, 104740 (2022).
15. Cao, L. *et al.* In silico prediction of influenza vaccine effectiveness by sequence analysis. *Vaccine* **39**, 1030–1034 (2021).
16. Guo, C. *et al.* Prediction of common epitopes on hemagglutinin of the influenza A virus (H1 subtype). *Exp. Mol. Pathol.* **98**, 79–84 (2015).
17. Peng, F., Xia, Y. & Li, W. Prediction of Antigenic Distance in Influenza A Using Attribute Network Embedding. *Viruses* **15**, 1478 (2023).
18. Shah, S. A. W. *et al.* Seasonal antigenic prediction of influenza A H3N2 using machine learning. *Nat. Commun.* **15**, 3833 (2024).
19. Zeller, M. A. *et al.* Machine Learning Prediction and Experimental Validation of Antigenic Drift in H3 Influenza A Viruses in Swine. *mSphere* **6**, e00920-20 (2021).
20. Jones, K. E. *et al.* Global trends in emerging infectious diseases. *Nature* **451**, 990–993 (2008).
21. McArthur, D. B. Emerging Infectious Diseases. *Nurs. Clin. North Am.* **54**, 297–311 (2019).
22. Zoonoses. *World Health Organization* https://www.who.int/news-room/fact-sheets/detail/zoonoses (2020).
23. Javanian, M. *et al.* A brief review of influenza virus infection. *J. Med. Virol.* **93**, 4638–4646 (2021).
24. Li, Y.-T., Linster, M., Mendenhall, I. H., Su, Y. C. F. & Smith, G. J. D. Avian influenza viruses in humans: lessons from past outbreaks. *Br. Med. Bull.* **132**, 81–95 (2019).
25. Glezen, W. P. Emerging Infections: Pandemic Influenza. *Epidemiol. Rev.* **18**, 64–76 (1996).
26. Kilbourne, E. D. Influenza Pandemics of the 20th Century. *Emerg. Infect. Dis.* **12**, 9–14 (2006).

27. Viboud, C. *et al.* Global Mortality Impact of the 1957–1959 Influenza Pandemic. *J. Infect. Dis.* **213**, 738–745 (2016).
28. Viboud, C. *et al.* Multinational Impact of the 1968 Hong Kong Influenza Pandemic: Evidence for a Smoldering Pandemic. *J. Infect. Dis.* **192**, 233–248 (2005).
29. Vandoorn, E. *et al.* Human Immunity and Susceptibility to Influenza A(H3) Viruses of Avian, Equine, and Swine Origin. *Emerg. Infect. Dis.* **29**, 98–109 (2023).
30. Yang, J. *et al.* Evolution of Avian Influenza Virus (H3) with Spillover into Humans, China. *Emerg. Infect. Dis.* **29**, (2023).
31. Petrova, V. N. & Russell, C. A. The evolution of seasonal influenza viruses. *Nat. Rev. Microbiol.* **16**, 47–60 (2018).
32. *Avian Influenza A(H5N2) - Mexico*. https://www.who.int/emergencies/disease-outbreak-news/item/2024-DON520#:~:text=On%2023%20May%202024%2C%20the,was%20hospitalized%20in%20Mexico%20City. (2024).
33. *Avian Influenza Overview September–December 2023*. https://www.ecdc.europa.eu/en/publications-data/avian-influenza-overview-september-december-2023 (2023).
34. *Communicable Disease Threats Report, 17-23 August 2024, Week 34*. https://www.ecdc.europa.eu/en/publications-data/communicable-disease-threats-report-17-23-august-2024-week-34 (2024).
35. *Cumulative Number of Confirmed Human Cases for Avian Influenza A(H5N1) Reported to WHO, 2003-2024, 19 July 2024*. https://www.who.int/publications/m/item/cumulative-number-of-confirmed-human-cases-for-avian-influenza-a(h5n1)-reported-to-who-2003-2024 (2024).
36. *Zoonotic Influenza - Annual Epidemiological Report for 2022*. https://www.ecdc.europa.eu/en/publications-data/zoonotic-influenza-annual-epidemiological-report-2022 (2023).
37. Suttie, A. *et al.* Inventory of molecular markers affecting biological characteristics of avian influenza A viruses. *Virus Genes* **55**, 739–768 (2019).
38. Dou, D., Revol, R., Östbye, H., Wang, H. & Daniels, R. Influenza A Virus Cell Entry, Replication, Virion Assembly and Movement. *Front. Immunol.* **9**, 1581 (2018).
39. Samji, T. Influenza A: understanding the viral life cycle. *Yale J. Biol. Med.* **82**, 153–159 (2009).
40. Du, R., Cui, Q. & Rong, L. Competitive Cooperation of Hemagglutinin and Neuraminidase during Influenza A Virus Entry. *Viruses* **11**, 458 (2019).
41. Russell, C. J., Hu, M. & Okda, F. A. Influenza Hemagglutinin Protein Stability, Activation, and Pandemic Risk. *Trends Microbiol.* **26**, 841–853 (2018).
42. Maines, T. R. *et al.* Effect of receptor binding domain mutations on receptor binding and transmissibility of avian influenza H5N1 viruses. *Virology* **413**, 139–147 (2011).
43. Decker, C. H., Rapier-Sharman, N. & Pickett, B. E. Mutation in Hemagglutinin Antigenic Sites in Influenza A pH1N1 Viruses from 2015–2019 in the United States Mountain West, Europe, and the Northern Hemisphere. *Genes* **13**, 909 (2022).
44. Opanda, S., Bulimo, W., Gachara, G., Ekuttan, C. & Amukoye, E. Assessing antigenic drift and phylogeny of influenza A (H1N1) pdm09 virus in Kenya using HA1 sub-unit of the hemagglutinin gene. *PLOS ONE* **15**, e0228029 (2020).
45. Yeo, J. Y. & Gan, S. K.-E. Peering into Avian Influenza A(H5N8) for a Framework towards Pandemic Preparedness. *Viruses* **13**, 2276 (2021).
46. Arthur, C. M., Cummings, R. D. & Stowell, S. R. Using glycan microarrays to understand immunity. *Curr. Opin. Chem. Biol.* **18**, 55–61 (2014).
47. Grant, O. C. *et al.* Combining 3D structure with glycan array data provides insight into the origin of glycan specificity. *Glycobiology* **26**, 772–783 (2016).
48. Grant, O. C. & Woods, R. J. Recent advances in employing molecular modelling to determine the specificity of glycan-binding proteins. *Curr. Opin. Struct. Biol.* **28**, 47–55 (2014).
49. Smith, D. F., Song, X. & Cummings, R. D. Use of Glycan Microarrays to Explore Specificity of Glycan-Binding Proteins. in *Methods in Enzymology* vol. 480 417–444 (Elsevier, 2010).
50. Topin, J. *et al.* Deciphering the Glycan Preference of Bacterial Lectins by Glycan Array and Molecular Docking with Validation by Microcalorimetry and Crystallography. *PLoS ONE* **8**, e71149 (2013).
51. Xu, R., McBride, R., Nycholat, C. M., Paulson, J. C. & Wilson, I. A. Structural Characterization of the

Hemagglutinin Receptor Specificity from the 2009 H1N1 Influenza Pandemic. *J. Virol.* **86**, 982–990 (2012).

52. Kawasaki, J., Tomonaga, K. & Horie, M. Large-scale investigation of zoonotic viruses in the era of high-throughput sequencing. *Microbiol. Immunol.* **67**, 1–13 (2023).
53. Pareek, C. S., Smoczynski, R. & Tretyn, A. Sequencing technologies and genome sequencing. *J. Appl. Genet.* **52**, 413–435 (2011).
54. Auewarakul, P. *et al.* An Avian Influenza H5N1 Virus That Binds to a Human-Type Receptor. *J. Virol.* **81**, 9950–9955 (2007).
55. Chen, L.-M. *et al.* In vitro evolution of H5N1 avian influenza virus toward human-type receptor specificity. *Virology* **422**, 105–113 (2012).
56. Chutinimitkul, S. *et al.* Virulence-Associated Substitution D222G in the Hemagglutinin of 2009 Pandemic Influenza A(H1N1) Virus Affects Receptor Binding. *J. Virol.* **84**, 11802–11813 (2010).
57. Gambaryan, A. *et al.* Evolution of the receptor binding phenotype of influenza A (H5) viruses. *Virology* **344**, 432–438 (2006).
58. Herfst, S. *et al.* Airborne Transmission of Influenza A/H5N1 Virus Between Ferrets. *Science* **336**, 1534–1541 (2012).
59. Naughtin, M. *et al.* Neuraminidase Inhibitor Sensitivity and Receptor-Binding Specificity of Cambodian Clade 1 Highly Pathogenic H5N1 Influenza Virus. *Antimicrob. Agents Chemother.* **55**, 2004–2010 (2011).
60. Stevens, J. *et al.* Structure and Receptor Specificity of the Hemagglutinin from an H5N1 Influenza Virus. *Science* **312**, 404–410 (2006).
61. Wang, W. *et al.* Glycosylation at 158N of the Hemagglutinin Protein and Receptor Binding Specificity Synergistically Affect the Antigenicity and Immunogenicity of a Live Attenuated H5N1 A/Vietnam/1203/2004 Vaccine Virus in Ferrets. *J. Virol.* **84**, 6570–6577 (2010).
62. Watanabe, Y. *et al.* Acquisition of Human-Type Receptor Binding Specificity by New H5N1 Influenza Virus Sublineages during Their Emergence in Birds in Egypt. *PLoS Pathog.* **7**, e1002068 (2011).
63. Yamada, S. *et al.* Haemagglutinin mutations responsible for the binding of H5N1 influenza A viruses to human-type receptors. *Nature* **444**, 378–382 (2006).
64. Yang, Z.-Y. *et al.* Immunization by Avian H5 Influenza Hemagglutinin Mutants with Altered Receptor Binding Specificity. *Science* **317**, 825–828 (2007).
65. Burke, D. F. & Smith, D. J. A Recommended Numbering Scheme for Influenza A HA Subtypes. *PLoS ONE* **9**, e112302 (2014).
66. Notredame, C. Recent progress in multiple sequence alignment: a survey. *Pharmacogenomics* **3**, 131–144 (2002).
67. Thompson, J. D., Higgins, D. G. & Gibson, T. J. CLUSTAL W: improving the sensitivity of progressive multiple sequence alignment through sequence weighting, position-specific gap penalties and weight matrix choice. *Nucleic Acids Res.* **22**, 4673–4680 (1994).
68. Edgar, R. C. MUSCLE: multiple sequence alignment with high accuracy and high throughput. *Nucleic Acids Res.* **32**, 1792–1797 (2004).
69. Edgar, R. C. & Batzoglou, S. Multiple sequence alignment. *Curr. Opin. Struct. Biol.* **16**, 368–373 (2006).
70. Gong, Z., Li, F. & Dong, L. Performance assessment of protein multiple sequence alignment algorithms based on permutation similarity measurement. *Biochem. Biophys. Res. Commun.* **399**, 470–474 (2010).
71. Edgar, R. C. MUSCLE user manual: Diagonal optimizations. (2004c).
72. Edgar, R. C. MUSCLE user manual: Save option. (2024e).
73. Almagro Armenteros, J. J. *et al.* SignalP 5.0 improves signal peptide predictions using deep neural networks. *Nat. Biotechnol.* **37**, 420–423 (2019).
74. Domingos, P. A few useful things to know about machine learning. *Commun. ACM* **55**, 78–87 (2012).
75. Reid Turner, C., Fuggetta, A., Lavazza, L. & Wolf, A. L. A conceptual basis for feature engineering. *J. Syst. Softw.* **49**, 3–15 (1999).
76. An, S.-H. *et al.* Improvement of PR8-Derived Recombinant Clade 2.3.4.4c H5N6 Vaccine Strains by Optimization of Internal Genes and H103Y Mutation of Hemagglutinin. *Vaccines* **8**, 781 (2020).
77. He, D. *et al.* Epidemiological investigation of infectious diseases in geese on mainland China during 2018–2021. *Transbound. Emerg. Dis.* **69**, 3419–3432 (2022).
78. Webster, R. G., Bean, W. J., Gorman, O. T., Chambers, T. M. & Kawaoka, Y. Evolution and ecology of influenza A viruses. *Microbiol. Rev.* **56**, 152–179 (1992).
79. Hiono, T. *et al.* Amino acid residues at positions 222 and 227 of the hemagglutinin together with the

neuraminidase determine binding of H5 avian influenza viruses to sialyl Lewis X. *Arch. Virol.* **161**, 307–316 (2016).

80. Seyer, R. *et al.* Synergistic Adaptive Mutations in the Hemagglutinin and Polymerase Acidic Protein Lead to Increased Virulence of Pandemic 2009 H1N1 Influenza A Virus in Mice. *J. Infect. Dis.* **205**, 262–271 (2012).
81. Shih, A. C.-C., Hsiao, T.-C., Ho, M.-S. & Li, W.-H. Simultaneous amino acid substitutions at antigenic sites drive influenza A hemagglutinin evolution. *Proc. Natl. Acad. Sci.* **104**, 6283–6288 (2007).
82. Chen, H., Zhou, X., Zheng, J. & Kwoh, C.-K. Rules of co-occurring mutations characterize the antigenic evolution of human influenza A/H3N2, A/H1N1 and B viruses. *BMC Med. Genomics* **9**, 69 (2016).
83. Pérez-Pérez, J. M., Candela, H. & Micol, J. L. Understanding synergy in genetic interactions. *Trends Genet.* **25**, 368–376 (2009).
84. Pedregosa, F., Varoquaux, G.¨l, Gramfort, A., Michel, V. & Thirion, B. Scikit-learn: Machine Learning in Python. *J. Mach. Learn. Res.* **12**, 2825–2830 (2011).
85. Alibrahim, H. & Ludwig, S. A. Hyperparameter Optimization: Comparing Genetic Algorithm against Grid Search and Bayesian Optimization. in *2021 IEEE Congress on Evolutionary Computation (CEC)* 1551–1559 (IEEE, Kraków, Poland, 2021). doi:10.1109/CEC45853.2021.9504761.
86. Liashchynskyi, P. & Liashchynskyi, P. Grid Search, Random Search, Genetic Algorithm: A Big Comparison for NAS. Preprint at https://doi.org/10.48550/ARXIV.1912.06059 (2019).
87. Hidayat, T. *et al.* Performance Prediction Using Cross Validation (GridSearchCV) for Stunting Prevalence. in *2024 IEEE International Conference on Artificial Intelligence and Mechatronics Systems (AIMS)* 1–6 (IEEE, Bandung, Indonesia, 2024). doi:10.1109/AIMS61812.2024.10512657.
88. API Reference - GridSearchCV.
89. LaValley, M. P. Logistic Regression. *Circulation* **117**, 2395–2399 (2008).
90. Nick, T. G. & Campbell, K. M. Logistic Regression. in *Topics in Biostatistics* (ed. Ambrosius, W. T.) vol. 404 273–301 (Humana Press, Totowa, NJ, 2007).
91. Bennett, K. P. & Campbell, C. Support vector machines: hype or hallelujah? *ACM SIGKDD Explor. Newsl.* **2**, 1–13 (2000).
92. Meyer, D. & Wien, F. T. Support vector machines. *R News* **1**, 23–26 (2001).
93. Chauhan, V. K., Dahiya, K. & Sharma, A. Problem formulations and solvers in linear SVM: a review. *Artif. Intell. Rev.* **52**, 803–855 (2019).
94. Kirasich, K., Smith, T. & Sadler, B. Random Forest vs Logistic Regression: Binary Classification for Heterogeneous Datasets. *SMU Data Sci. Rev.* **1**, (2018).
95. More, A. S. & Rana, D. P. Review of random forest classification techniques to resolve data imbalance. in *2017 1st International Conference on Intelligent Systems and Information Management (ICISIM)* 72–78 (IEEE, Aurangabad, 2017). doi:10.1109/ICISIM.2017.8122151.
96. Zhang, H., Zimmerman, J., Nettleton, D. & Nordman, D. J. Random Forest Prediction Intervals. *Am. Stat.* **74**, 392–406 (2020).
97. Chen, T. & Guestrin, C. XGBoost: A Scalable Tree Boosting System. in *Proceedings of the 22nd ACM SIGKDD International Conference on Knowledge Discovery and Data Mining* 785–794 (ACM, San Francisco California USA, 2016). doi:10.1145/2939672.2939785.
98. Li, W., Yin, Y., Quan, X. & Zhang, H. Gene Expression Value Prediction Based on XGBoost Algorithm. *Front. Genet.* **10**, 1077 (2019).
99. Berrar, D. Cross-validation. *Encycl. Bioinforma. Comput. Biol. 2nd Ed. Elsevier* 542–545 (2019).
100. Xu, Y. & Goodacre, R. On Splitting Training and Validation Set: A Comparative Study of Cross-Validation, Bootstrap and Systematic Sampling for Estimating the Generalization Performance of Supervised Learning. *J. Anal. Test.* **2**, 249–262 (2018).
101. Vujovic, Ž. Đ. Classification Model Evaluation Metrics. *Int. J. Adv. Comput. Sci. Appl.* **12**, (2021).
102. Naidu, G., Zuva, T. & Sibanda, E. M. A Review of Evaluation Metrics in Machine Learning Algorithms. in *Artificial Intelligence Application in Networks and Systems* (eds. Silhavy, R. & Silhavy, P.) vol. 724 15–25 (Springer International Publishing, Cham, 2023).
103. Rainio, O., Teuho, J. & Klén, R. Evaluation metrics and statistical tests for machine learning. *Sci. Rep.* **14**, 6086 (2024).
104. Rajbahadur, G. K., Wang, S., Oliva, G. A., Kamei, Y. & Hassan, A. E. The Impact of Feature Importance Methods on the Interpretation of Defect Classifiers. *IEEE Trans. Softw. Eng.* **48**, 2245–2261 (2022).
105. Wu, N. C. *et al.* Diversity of Functionally Permissive Sequences in the Receptor-Binding Site of Influenza

Hemagglutinin. *Cell Host Microbe* **21**, 742-753.e8 (2017).

106. De Vries, R. P. *et al.* Three mutations switch H7N9 influenza to human-type receptor specificity. *PLOS Pathog.* **13**, e1006390 (2017).
107. Vogel, O. A. & Manicassamy, B. Broadly Protective Strategies Against Influenza Viruses: Universal Vaccines and Therapeutics. *Front. Microbiol.* **11**, 135 (2020).